

## Designed Nucleotide Binding Motifs

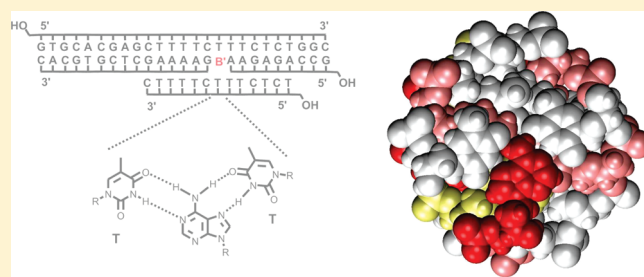
Christoph Kröner,<sup>†</sup> Manuel Röthlingshöfer,<sup>‡</sup> and Clemens Richert<sup>\*†</sup>

<sup>†</sup>Institute for Organic Chemistry, University of Stuttgart, 70569 Stuttgart, Germany

<sup>‡</sup>Institute for Organic Chemistry, University of Karlsruhe/K.I.T., 76131 Karlsruhe, Germany

**S** Supporting Information

**ABSTRACT:** Gaps in the central strand of oligonucleotide triplexes bind nucleoside phosphates tightly. Watson–Crick and Hoogsteen base pairing as design principle yield motifs with high affinity for nucleoside phosphates with A or G as nucleobase, including ATP. The second messenger 3',5'-cAMP is bound with nanomolar affinity. A designed DNA motif accommodates seven nucleotides at a time. The design was implemented for both DNA and RNA.



All biological cells contain mono-, di-, and triphosphates of nucleosides and use them as substrates, components of cofactors, signaling molecules, and energy sources for enzymatic reactions. As a consequence, there is a keen interest in binding motifs for nucleoside phosphates. Synthetic receptors for nucleoside phosphates that can act as sensors include azacrown ethers,<sup>1</sup> transition-metal complexes,<sup>2</sup> and polymers.<sup>3</sup> Several RNA sequence motifs that bind nucleotides have been identified by systematic evolution of ligands by exponential enrichment (SELEX).<sup>4–6</sup> This includes aptamers for ATP,<sup>7–11</sup> GTP,<sup>12</sup> coenzyme A,<sup>13</sup> and S-adenosyl methionine.<sup>14,15</sup> Cationic building blocks give aptamers with increased specificity.<sup>16,17</sup> An aptamer that binds cAMP with 10  $\mu$ M dissociation constant has also been reported.<sup>18</sup> Fusing nucleotide-specific aptamers and ribozymes can produce aptazymes whose catalytic activity is modulated by nucleotide concentration in allosteric fashion.<sup>19</sup> Aptazymes have also been reported for cAMP, cCMP, and cGMP.<sup>20–22</sup>

Changing the specificity of aptamers from one nucleotide to another can be difficult, though, and a change in specificity from ATP to GTP involved a mutation rate of 24%.<sup>12</sup> Also, there is no obvious approach for generating aptamers that bind several nucleotides at a time without multiplying the motif itself. Further, nucleotide-binding aptamers composed of DNA<sup>23</sup> are rare, which is unfortunate, as synthetic oligodeoxynucleotides are less expensive than oligoribonucleotides. Finally, the disassembly of nucleotide binding motifs and the controlled release of the nucleoside phosphates are not trivial to program when complex, folded unimolecular structures are involved.

An interest in developing ATP storage devices prompted us to study nucleotide binding motifs that are based on inexpensive synthetic oligodeoxynucleotides and that assemble via designed, canonical base pairing. Here we report a four-strand system based on a DNA triple helix whose specificity is readily switched from A to G and can bind more than one nucleotide at a time. It

binds cAMP with nanomolar affinity, i.e., more tightly than the known aptamer<sup>18</sup> or allosteric ribozyme.<sup>24</sup>

Figure 1 shows the first binding motif tested (I). It consists of four strands that together form an interrupted triplex with a single nucleotide gap in the oligopurine strand. This gap can accommodate a nucleotide. The motif was designed such that three distinct transitions could be expected in UV–melting curves: one for the release of the triplex-forming oligonucleotide (TFO) and one each for the disassembly of the shorter and the longer duplex. The experimental melting profile showed all three transitions (Figure 2a). Upon addition of adenosine 5'-triphosphate (ATP), only the triplex transition showed a significant shift, with a  $\Delta T_m$  of 8.2 °C, i.e., more than the increase typically seen for extension of a triplex by three nucleotides. This suggests that the triplex motif binds the triphosphate tightly at micromolar concentration. Since the nucleotide should be the more weakly binding component, the shift in the transition also suggests that TFO and nucleotide dissociate from the remaining complex simultaneously.

A range of different adenosine phosphates were then tested as ligands for I (Figure 2b, Table 1). All induced melting point increases. At high magnesium concentration, dATP produced a greater shift in the triplex melting point than other nucleotides, while in the absence of  $Mg^{2+}$  dAMP was bound most tightly. An exceptionally large  $\Delta T_m$  (+16 °C) identified the cyclic mononucleotide 3',5'-cAMP as a particularly good ligand. Neither of the nucleoside phosphates with a mismatched nucleobase (C, G, T) showed any significant effect on the triplex transition (see also Table S1, Supporting Information).

We then redesigned the motif to bind guanosine phosphates by changing the ligand-pairing nucleobases from T to C. The

Received: February 10, 2011

Published: March 17, 2011

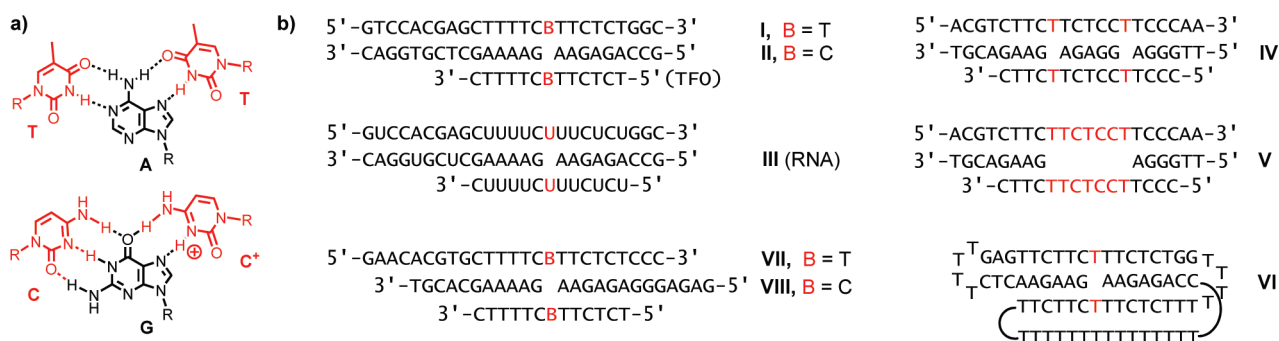


**Figure 1.** Binding motifs: (a) base pairing in the recognition pocket; (b) sequences employed. Nucleobases designed to pair with the target nucleotide are shown in red.

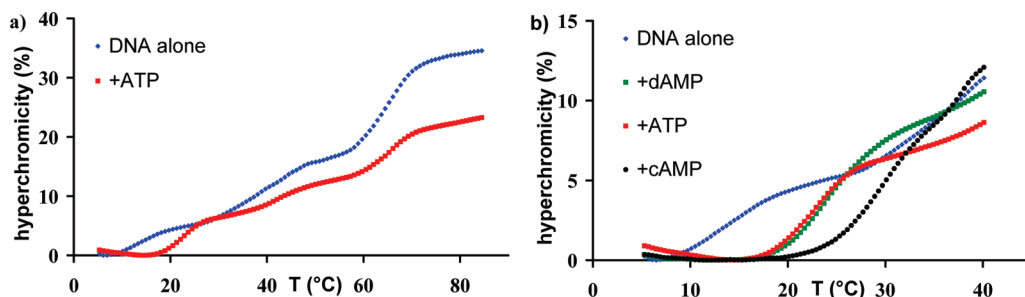


**Figure 2.** UV-melting profiles of motif I: (a) full melting curve in the presence or absence of ATP (note that the addition of 10 equivalents of ligand lowers the overall hyperchromicity); (b) expanded region showing triplex melting, in the absence or presence of nucleotides. Conditions: 1  $\mu$ M oligonucleotides, 10  $\mu$ M nucleotide, 10 mM phosphate buffer, pH 7.0, 1 M NaCl, 80 mM  $\text{MgCl}_2$ .

resulting motif (II) now showed melting point increases for G as base (Table 1), confirming that the most likely interaction is Watson-Crick and Hoogsteen base pairing. The  $\Delta T_m$  value observed for dGMP (+10  $^\circ\text{C}$ ) is respectable, given that the melting curve experiments were performed at pH 7.0, i.e., above the more acidic buffers favoring the protonation of the central C in the TFO that is required for Hoogsteen base pairing.<sup>25</sup>

We then performed UV-melting studies with an RNA version of motif I (motif III). Annealing led to a complex whose triplex transition was too low to be accurately measured in the absence of a nucleotide. In the presence of adenosine phosphates, a shift to observable triplex transitions was observed, even though the pH was again fixed to a value that is physiologically relevant but not optimal for the C:G:C<sup>+</sup> base triplets in the core regions of the motif (Table 2). Triplex stabilization was again specific for A as nucleobase, with a significantly lower  $\Delta T_m$  in the presence of dGMP and no detectable stabilization in the presence of dCMP or dTMP.

Next, we asked whether the designed motif can bind more than one nucleotide at a time. Motif IV contains two gaps in the central strand of the triplex. Again, an increase in the triplex melting point was observed upon addition of cAMP (Figure 3). Two equivalents gave a more pronounced stabilization than 1 equiv, and the stabilizing effect leveled off as the concentration was increased further. When motif V with its seven-nucleotide wide gap was incubated with a mixture of cAMP and cGMP (10  $\mu$ M each), a melting point increase of 5.5  $^\circ\text{C}$  was measured (Table 1), again suggesting that binding of nucleotides was occurring.

We then designed intramolecular folding motif VI, whose binding pocket includes the 3'- and 5'-termini of the sequence.

Melting curves again showed individual transitions for the dissociation of the triplex and duplex regions (Figure S8, Supporting Information). The triplex transition was shifted by +17.5  $^\circ\text{C}$  in the case of cAMP (Table 1).

Finally, absorption measurements from filtration assays gave dissociation constants for representative complexes between oligonucleotides and nucleoside phosphates (Table 3). For this, the length of two of the strands of motif I was changed to minimize the elution of residual oligonucleotides through the filtration membrane. The values given in Table 3 are upper limits of the dissociation constants, as neither partial dissociation during the centrifugation nor traces of oligonucleotides in the eluate can be ruled out. Even so, low micromolar (ATP) or nanomolar (cAMP) dissociation constants were found for the cognate nucleotides, while nucleotides with a noncomplementary nucleobase gave little or no detectable binding (motif VII and cGMP, TMP, dCMP, UMP, see Table S5, Supporting Information). When the central two purine-rich strands of motif VII were replaced with a continuous strand that does not leave a gap for nucleotide binding, the ability to bind cAMP disappears (Figure S12, Supporting Information). The same is true for a version of motif I with continuous central strand. Its melting point does not change upon addition of cAMP (Figure S13, Supporting Information). Again, this demonstrates that the designed binding pocket is indeed where the nucleotide binds.

For motifs IV and V, the stoichiometry of complex formation is not 1:1, so that true binding or dissociation constants have other dimensions than  $\text{M}^{-1}$ . Ignoring this fact, apparent dissociation constants of 14.2  $\mu\text{M}$  (IV, cAMP) and 177  $\mu\text{M}$  (V, cAMP plus cGMP) are obtained from the absorption measurements (Tables S7 and S8, Supporting Information).

**Table 1. Triplex Melting Points<sup>a</sup> (°C) of Sequence Motifs I, II, V, and VI in the Absence or Presence of Nucleotides<sup>b</sup>**

motif	nucleotide	MgCl <sub>2</sub> (80 mM)		no MgCl <sub>2</sub>	
		T <sub>m</sub>	ΔT <sub>m</sub> <sup>c</sup>	T <sub>m</sub>	ΔT <sub>m</sub> <sup>c</sup>
I		14.0		<10	
I	dAMP	23.9	9.9	22.6	>12.6
I	dATP	26.0	12.0	15.9	>5.9
I	AMP	20.5	6.5	17.5	>7.5
I	ADP	22.3	8.3	15.0	>5.0
I	ATP	22.2	8.2	13.8	>3.8
I	cAMP	30.0	16.0	26.8	>16.8
I	dGMP	14.0	0	10	0
I	TMP	14.0	0	<10	
I	dCMP	12.0	-2.0	<10	
II		14.0		<10	
II	dGMP	24.0	10.0	22.4	>12.4
II	dGTP	19.5	5.5	10.6	
II	GMP	15.0	1.0	12.5	>2.5
II	GDP	15.2	1.2	10.4	
II	GTP	15.3	1.3	10.2	
II	dAMP	12.0	-2.0	10.8	
II	TMP	14.0	0	10.5	
II	dCMP	13.0	-1.0	10.4	
V				16.0 <sup>d</sup>	
V	cAMP				
V	+ cGMP <sup>e</sup>	n.d.		21.5 <sup>d</sup>	5.5
VI		n.d.		14.3	
VI	cAMP	n.d.		31.8	17.5

<sup>a</sup> Mean of two melting curves. <sup>b</sup> Conditions: 1 μM oligonucleotides, 10 μM nucleotide, 10 mM phosphate buffer, pH 7.0, 1 M NaCl, except for motif V. <sup>c</sup> To triplex in the absence of ligand. <sup>d</sup> Buffer: 20 mM Tris.HCl, pH 6.7, 450 mM NaCl, 100 mM KCl, 10 mM MgCl<sub>2</sub>, 1 mM MnCl<sub>2</sub>, 5 mM CaCl<sub>2</sub>. <sup>e</sup> 10 μM of either nucleotide.

**Table 2. Triplex Melting Points<sup>a</sup> for RNA Sequence Motif III in the Presence or Absence of Nucleoside Phosphates**

nucleotide	T <sub>m</sub> (°C)	ΔT <sub>m</sub> <sup>b</sup> (°C)
	<10.0	
ATP	15.5	>5.5
ADP	16.1	>6.1
AMP	17.1	>7.1
dATP	16.8	>6.8
dAMP	18.5	>8.5
dGMP	11.8	>1.8
TMP	<10.0	
dCMP	<10.0	

<sup>a</sup> Mean of two melting curves at 5 μM oligonucleotides, 50 μM nucleotide, 10 mM phosphate buffer, pH 7.0, 1 M NaCl, 80 mM MgCl<sub>2</sub>. <sup>b</sup> To triplex melting point without ligand.

Our results show that DNA-based triplex motifs bind nucleoside phosphates of both the deoxy and ribo series at micromolar concentrations. The order of affinity may, in part, be explained by the fact that the cyclic nucleotides cAMP and cGMP have the least steric demand and feature a phosphodiester, rather than a

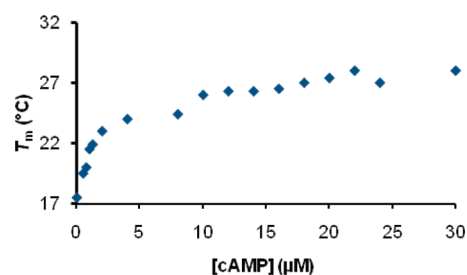


**Figure 3.** Melting points of the triplex in IV at different cAMP concentrations (1 μM IV, 10 mM phosphate, pH 7.0, 1 M NaCl). Note that the T<sub>m</sub> increase begins to level off at 2 equiv of the nucleotide.

**Table 3. Dissociation Constants<sup>a</sup> for Complexes between Motifs VI–VIII and Nucleotides, As Determined in Filtration Assays**

motif	buffer <sup>b</sup>	nucleotide	K <sub>d</sub> (μM)
VI	A	cAMP	1.5
VII	A	cAMP	0.3
VII	B	cAMP	<0.3
VII	A	ATP	4
VIII	C	cGMP	30

<sup>a</sup> At 4 °C. <sup>b</sup> Buffers: (A) 10 mM phosphate buffer, pH 7.0, 1 M NaCl; (B) 20 mM Tris.HCl, pH 6.7, 450 mM NaCl, 100 mM KCl, 10 mM MgCl<sub>2</sub>, 1 mM MnCl<sub>2</sub>, 5 mM CaCl<sub>2</sub>; (C) 10 mM phosphate buffer, pH 6.2, 200 mM KCl, 5 mM MgCl<sub>2</sub>, 0.1 mM EDTA. See the Supporting Information for further details.

monoester group. The latter can dissociate twice, leading to a (partially) doubly negatively charged phosphate group, whereas the former can dissociate only once.

Physiologically relevant intramolecular triplexes are known.<sup>26</sup> The designed binding motifs also bear some similarity to adenine- and guanine-binding riboswitches that regulate gene expression. The riboswitches use Watson–Crick base pairing in the recognition of ligands,<sup>27</sup> but do not employ conventional Hoogsteen base pairing, and fully engulf their target bases, creating a binding pocket too small for nucleoside phosphates.

Aptazymes and riboswitches respond to changes in ligand concentration, and our results point to possible applications of triplex motifs as sensor or chemical biology tools. But, more importantly, our results also show that one triplex motif can bind several nucleoside phosphates at a time and release them upon gentle heating.

Nucleoside phosphates are linked to energy in the cell. The ability to harvest energy-rich compounds and releasing them, in the form of mechanical work or heat, at a different time and/or place, again without the use of fossil fuel, and without environmental pollution, is directly linked to the energy challenge of a sustainable planet. It is therefore significant how easily ATP-binding DNA sequence motifs can be designed and generated from commercially available oligonucleotides. Since a number of small DNA triplexes are known whose three-dimensional structure has been solved,<sup>28</sup> our results also point to opportunities in the design of other binding motifs for nucleoside phosphates.

## EXPERIMENTAL SECTION

**UV–Melting Experiments.** Melting curves were recorded at 260 nm. The samples were prepared in quartz cuvettes with 10 or 2 mm path length. The oligonucleotides of the binding motif were either 1



or 5  $\mu\text{M}$  in the given buffer. Mononucleotide concentrations ranged from 0.2 to 50  $\mu\text{M}$ , as stated for the individual assays. The rate of heating was 1  $^{\circ}\text{C}/\text{min}$ . A modest level of hysteresis was observed in some cooling curves that all but disappeared when cooling at a rate of 0.2  $^{\circ}\text{C}/\text{min}$ . For the determination of melting points, heating curves were used exclusively. Melting points were calculated as the maxima of the first derivatives of the 95 point-smoothed melting curves, using UV WinLab 3.0 software of the spectrophotometers.

**Filtration Assays.** Solutions of oligonucleotides forming the binding motif (500  $\mu\text{L}$ , 10  $\mu\text{M}$ ) and the nucleotide (5, 10, 20, or 70  $\mu\text{M}$ ) were prepared in the buffer of choice. The solutions were vortexed and heated to 95  $^{\circ}\text{C}$  for 5 min. Annealing was induced by allowing the solution to cool from 95 to 4  $^{\circ}\text{C}$  in 2 h. The samples were transferred to Amicon Ultra filter devices (3 kDa cutoff). The filtration was performed at 4  $^{\circ}\text{C}$  and 13000g for 1 h. To the filtrate (450  $\mu\text{L}$ ) was added buffer to give a final volume of 600  $\mu\text{L}$ . The absorption of the resulting solution was measured in the range of 200–400 nm. The concentration of the eluted mononucleotide was calculated according to Lambert–Beer's law (extinction coefficients at 260 nm: cAMP 12300  $\text{M}^{-1}\text{cm}^{-1}$ ; ATP 15400  $\text{M}^{-1}\text{cm}^{-1}$ ; cGMP 13600  $\text{M}^{-1}\text{cm}^{-1}$ ; TMP 9700  $\text{M}^{-1}\text{cm}^{-1}$ , dCMP 9100  $\text{M}^{-1}\text{cm}^{-1}$ ; UMP 10000  $\text{M}^{-1}\text{cm}^{-1}$ ).<sup>29</sup> For the determination of the dissociation constants, it was assumed that all unbound mononucleotides are eluted through the membrane and that the off-rate is slow compared to the time scale of the filtration. It was also assumed that the absorption in the eluate is caused by nucleotides only, as control experiments with just the oligonucleotides did not show significant absorption. Since either of these assumptions are for ideal assay conditions, the dissociation constants reported are believed to be at the upper limit of the true values (i.e., binding may, in fact, be tighter than reported).

## ■ ASSOCIATED CONTENT

**Supporting Information.** Reagents, additional melting data, spectra used for determining dissociation constants, and simulated binding curves. This material is available free of charge via the Internet at <http://pubs.acs.org>.

## ■ AUTHOR INFORMATION

### Corresponding Author

\*Tel: int-49 (0) 711 608 64311. Fax: int-49 (0) 711 608 64321. E-mail: [lehrstuhl-2@oc.uni-stuttgart.de](mailto:lehrstuhl-2@oc.uni-stuttgart.de).

## ■ ACKNOWLEDGMENT

We thank Prof. U. E. Steiner for simulated binding curves, Dr. H. Rudolph for access to a centrifuge, and Dr. E. Kervio for discussions. This work was supported by DFG (grant RI 1063/9-1) and the University of Stuttgart.

## ■ REFERENCES

- (1) Bazzicalupi, C.; Bencini, A.; Biagini, S.; Faggi, E.; Meini, S.; Giorgi, C.; Spepi, A.; Valtancoli, B. *J. Org. Chem.* **2009**, *74*, 7349–7363.
- (2) Nair, A. K.; Neelakandan, P. P.; Ramaiah, D. *Chem. Commun.* **2009**, *42*, 6352–6354.
- (3) Yao, Z.; Feng, X.; Hong, W.; Li, C.; Shi, G. *Chem. Commun.* **2009**, *31*, 4696–4698.
- (4) Ellington, A. D.; Szostak, J. W. *Nature* **1990**, *346*, 818–822.
- (5) Famulok, M.; Hartig, J. S.; Mayer, G. *Chem. Rev.* **2007**, *107*, 3715–3743.
- (6) Fiammengo, R.; Jäschke *Curr. Opin. Biotech.* **2005**, *16*, 614–621.
- (7) Sasanfar, M.; Szostak, J. W. *Nature* **1993**, *364*, 550–553.

- (8) Jiang, F.; Kumar, R. A.; Jones, R. A.; Patel, D. J. *Nature* **1996**, *382*, 183–186.
- (9) Dieckmann, T.; Suzuki, E.; Nakamura, G. K.; Feigon, J. *RNA* **1996**, *2*, 628–640.
- (10) Sazani, P. L.; Larralde, R.; Szostak, J. W. *J. Am. Chem. Soc.* **2004**, *126*, 8370–8371.
- (11) Weill, L.; Louis, D.; Sargueil, B. *Nucleic Acids Res.* **2004**, *32*, 5045–5058.
- (12) Huang, Z.; Szostak, J. W. *RNA* **2003**, *9*, 1456–1463.
- (13) Saran, D.; Frank, J.; Burke, D. H. *BMC Evol. Biol.* **2003**, *3*, 26–37.
- (14) Burke, D. H.; Gold, L. *Nucleic Acids Res.* **1997**, *25*, 2020–2024.
- (15) Burgstaller, P.; Famulok, M. *Angew. Chem., Int. Ed. Engl.* **1994**, *33*, 1084–1087.
- (16) Battersby, T. R.; Ang, D. N.; Burgstaller, P.; Jurczyk, S. C.; Bowser, M. T.; Buchanan, D. D.; Kennedy, R. T.; Benner, S. A. *J. Am. Chem. Soc.* **1999**, *121*, 9781–9789.
- (17) Vaish, N. K.; Larralde, R.; Fraley, A. W.; Szostak, J. W.; McLaughlin, L. W. *Biochemistry* **2003**, *42*, 8842–8851.
- (18) Koizumi, M.; Breaker, R. R. *Biochemistry* **2000**, *39*, 8983–8992.
- (19) Tang, J.; Breaker, R. R. *Chem. Biol.* **1997**, *4*, 453–459.
- (20) Koizumi, M.; Soukup, G. A.; Kerr, J. N. Q.; Breaker, R. R. *Nat. Struct. Biol.* **1999**, *6*, 1062–1071.
- (21) Soukup, G. A.; Breaker, R. R. *Curr. Opin. Struct. Biol.* **2000**, *10*, 318–325.
- (22) Micura, R. *Angew. Chem.* **2006**, *118*, 32–34.
- (23) Huizenga, D. E.; Szostak, J. W. *Biochemistry* **1995**, *34*, 656–665.
- (24) Soukup, G. A.; Derose, E. C.; Koizumi, M.; Breaker, R. R. *RNA* **2001**, *7*, 524–536.
- (25) Thuong, N. T.; Hélène, C. *Angew. Chem., Int. Ed. Engl.* **1993**, *32*, 666–690.
- (26) Mitton-Fry, R. M.; DeGegorio, S. J.; Wang, J.; Steitz, T. A.; Steitz, J. A. *Science* **2010**, *330*, 1244–1247.
- (27) (a) Mandal, M.; Breaker, R. R. *Nat. Struct. Mol. Biol.* **2004**, *11*, 29–35. (b) Serganov, A.; Yuan, Y. R.; Pikoyskaya, O.; Polonskaia, A.; Malinina, L.; Phan, A. T.; Höbartner, C.; Micura, R.; Breaker, R. R.; Patel, D. J. *Chem. Biol.* **2004**, *11*, 1729–1741. (c) Noeske, J.; Richter, C.; Grundl, M. A.; Nasiri, H. R.; Schwalbe, H.; Wohnert, J. *Proc. Natl. Acad. Sci. U.S.A.* **2005**, *102*, 1372–1377.
- (28) (a) Radhakrishnan, I.; Patel, D. J. *Structure* **1993**, *1*, 135–152. (b) Betts, L.; Josey, J. A.; Veal, J. M.; Jordan, S. R. *Science* **1995**, *270*, 1838–1841. (c) Vlieghe, D.; Van Meervelt, L.; Dautant, A.; Gallois, B.; Precigoux, G.; Kennard, O. *Science* **1996**, *273*, 1702–1705. (d) Gottfredsen, C. H.; Schultze, P.; Feigon, J. *J. Am. Chem. Soc.* **1998**, *120*, 4281–4289. (e) Asensio, J. L.; Brown, T.; Lane, A. N. *Nucleic Acids Res.* **1998**, *26*, 3677–3686. (f) Rhee, S.; Han, Z.; Liu, K.; Miles, H. T.; Davies, D. R. *Biochemistry* **1999**, *38*, 16810–16815. (g) Sussman, D.; Nix, J. C.; Wilson, C. *Nat. Struct. Biol.* **2000**, *7*, 53–57. (h) Sorensen, J. J.; Nielsen, J. T.; Petersen *Nucleic Acids Res.* **2004**, *32*, 6078–6085. (i) Petersson, P. E.; Nielsen, B. B.; Rasmussen, H.; Larsen, I. K.; Gajhede, M.; Nielsen, P. E.; Kastrup, J. S. *J. Am. Chem. Soc.* **2005**, *127*, 1424–1430.
- (29) Lang, L. *Absorption Spectra in the Ultraviolet and Visible Region*; Academic Press: New York, 1966.